to be presented at the International Conference on Pressure Vessel Technology and 1996 ASME Pressure Vessel and Piping Division Conference, Montreal, Quebec, Canada, July 20-27, 1996.

RESIDUAL STRESSES AND RETAINED AUSTENITE DISTRIBUTION AND EVOLUTION IN SAE 52100 STEEL UNDER ROLLING CONTACT LOADING

Ricardo C. Dommarco
INTEMA Univ Nac Mar del Plata
Av J.B.Justo 4302
7600 Mar del Plata, Argentina

Krzysztof J. Kozaczek
HTML,Oak Ridge Nat. Lab.,
Oak Ridge, Tennessee,
37831, USA.

Pedro C. Bastias George T. Hahn Carol A. Rubin
Mechanical Engineering Department, Vanderbilt University
Nashville, TN 37205, USA

ABSTRACT

Residual stresses are introduced and modified during manufacturing and also by normal use. In this paper the changes in magnitude and distribution of residual stresses, attending the strain induced transformation of retained austenite are examined. Tests were conducted on SAE 52100 bearing steel with different amounts of retained austenite in a 5-ball-rod rolling contact fatigue machine. The tests were accelerated by applying well-controlled micro-indentations on the wear track and using rough balls. The magnitude and distribution of residual stresses and retained austenite were measured using x-ray diffraction techniques. The contribution of the residual stresses and amount of retained austenite to the rolling contact fatigue life is analyzed.

1. INTRODUCTION

The residual stresses (RS) present in components to be subjected to rolling contact fatigue (RCF) can be introduced by different thermo-mechanical treatments (Maeda and Tsushima, 1994; Barski, 1994; Voskamp, 1986). The sign and magnitude of stresses are affected by a large number of variables such as geometry of the component, loading rate, temperature, lubrication, manufacturing techniques, heat treatments, etc. These stresses are altered by the plastic deformation and stress or strain induced phase transformation which takes place under service loads (Voskamp, 1994). The amount of retained austenite (RA) present in the heavily stressed region under the raceway of bearing steels decreases due to the action of repeated cyclic loading (Tricot et al., 1972; Voskamp et al., 1980; Yajima et al., 1974). The kinetics of martensite decay has been related to the formation of dark etching regions (DER) and later of white etching bands (WEB) (Voskamp et al., 1980). These bands have been shown to be formed of ferrite micro bands separated by regions of the original martensitic structure (Swahn et al., 1976; Österlund and Vingsbo, 1980). Large compressive RS develop in the circumferential (Voskamp et al., 1980; Zwirlein and Schlicht, 1982; Voskamp, 1985) and axial directions (Zwirlein and Schlicht, 1982) w.r.t. the raceway due to rolling contact loading. Maximum values of compressive circumferential residual stresses as high as σ'_c = -500 to -800 MPa (Voskamp et al., 1980) and σ'_c = -600 to -900 MPa (Zwirlein and Schlicht, 1982) have been reported for contact pressures of p_o = 3.3 and 3.0 GPa, respectively. These RS have been used (Zwirlein and Schlicht, 1982) to explain the presence and orientation features of WEBs in bearing steels. It has been observed (Schlicht et al., 1988) that in stabilized (bainitic) bearing steels the compressive residual stresses vary from an initial σ^r = -200 MPa to σ^r = -500 MPa after N = 10^6 cycles. However, these steels do not present a significant amount of RA among their microstructural constituents. Work conducted in pinion gears made out of (i) carbonitrided-oil quenched, and (ii) carbonitrided-oil quenched-shot-peened materials, with 30-35% and 5-7% RA at the surface respectively, revealed that the progressive RA transformation into martensite (γ-α')is not directly coupled with the variation of RS (Batista et al., 1994; Castanhola Batista et al., 1993). The former varies significantly during the first 30 hours of operation and the latter has reached a steady state before five hours of testing. Eventually, though, a shakedown state (Johnson and Jeffries, 1963) is reached.

2. EXPERIMENTAL PROCEDURE

2.1. Rolling Contact Fatigue Experiments

RCF tests were conducted in a ball-rod rolling contact fatigue tester (Glover, 1982). The standard three balls and a retainer arrangement was replaced by five balls without a retainer (Liston, 1995). As a consequence of this change the number of stress cycles per revolution of the specimen increased from 2.39 to 3.98 cycles/rev. The 9.53 mm (3/8") diameter specimen rotates at 3600 rpm and is lubricated by 8-10 drops per minute of Exxon 2380 turbo oil. The material used for the evaluation was steel SAE 52100; Table I indicates its chemical composition. Table II shows the different heat treatments applied to the specimens, and the resulting surface hardness. The specimens were loaded by SAE 52100 rough balls (RB), i.e. surface roughness 0.11 μm (4.28 AA). The tests were conducted at a peak pressure of p_o = 3600 MPa. According to Hertzian (elastic) theory this pressure produces an elliptical contact patch with minor and major contact lengths equal to: 2a= 313μm, and 2b= 549μm, respectively. This gives a

relation a/b=0.57 and was used to calculate the minor axis 2a, by measuring the major contact length 2b, which coincides with the wear track width. The major axis, transverse to the rolling direction (RD), was measured to be around 2b = 650 μm for all samples at 10^6 contacts, and the minor axis, oriented in the RD, was estimated to be 2a = 370 μm. The operating temperature of the balls-rod assembly was measured as T = 75°C. Artificial defects (AD) were placed on the wear track by using a Rockwell-C indentor, the load was controlled to produce uniform hemispherical indentations with 120 μm diameters. The presence of AD on the wear track accelerates the qualitative evaluation of the RCF properties of materials. The specimens were loaded until failure, i.e. spalling, took place. The tests were automatically stopped once a certain vibration threshold was detected by an accelerometer. A total of ten tests were conducted over each sample. The fatigue test results were analyzed using a two-parameter Weibull statistic and the L_{10} and L_{50} lives were evaluated.

2.2. X-Ray Measurements

A Scintag 4-axis goniometer with the x-ray tube operating a 45 kV/40 mA and Scintag solid state detector were used for the measurements. The radius of the focusing circle was 290 mm. The incident x-ray beam was collimated by a double pinhole collimator with 0.5 mm aperture and a divergence of approximately 0.1°. Cu K_α radiation was used for the RA measurements. Cr K_α radiation was used for RS measurements. The goniometer was aligned and calibrated using LaB_6 powder (NIST SRM 660). All peaks were fit with a symmetric Pearson VII function with a linear background correction and no Lorentz-Polarization-Absorption correction using the Scintag DMS 2000 software, Rev. 2.90. The least-square estimate of profile fit to LaB_6 powder peak in the range of ψ tilts from -45 to -45° was better than 0.002° of 2θ (θ is the Bragg angle).

2.2.1. Retained Austenite Analysis/ The retained austenite content was determined by an x-ray diffraction technique on selected wear tracks at different depths. Since chromium radiation could not be used, due to the large width of the diffraction peaks, Cu K_α radiation and a cylindrical collimator 0.5mm in diameter and 10 cm in length were employed. This radiation penetrates approximately 1.5 μm (63% of the information comes from this layer, which is known as the τ penetration depth). For the analysis, the (200) austenite peak at approximately 2θ = 75° and the martensite doublet (211)(112) at 2θ = 82° were used. A scan of 6° was done around each peak with a 2θ step of 0.05° and a collection time of 10 seconds/point. The analysis of retained austenite was carried out using the algorithm described in (Cullity, 1978).

2.2.2. Residual Stress Measurements/ Residual stress measurements in the martensite were done on all wear tracks at different depths (surface material was sequentially removed by chemical etching in 85 parts of distilled water, 10 parts of hydrofluoric acid and 15 parts of hydrogen peroxide). The standard chi-tilt (Noyan and Cohen, 1987) technique was used with 7 equi-$\sin^2\psi$ tilts from ψ=-45° to ψ=+45° in two perpendicular directions (hoop and axial). Cr K_α radiation was used providing for a τ penetration depth of 4.5 μm at ψ=0°. The 2θ position of the martensite (211-112) reflection was approximately 155.5°, and the peak width was approximately 10°. A 2θ range from 150° to 161° was scanned with the step size of 0.06° and data collection times of 10-15 seconds step.

The least-squares profile fit estimated error in 2θ due to the counting statistics was in the range 0.03-0.09°. A plane stress (biaxial) condition was assumed at each tested depth, and the unstressed lattice spacing d_o was calculated using the Hauk-Döle method (Dölle and Hauk, 1977). The correctness of the d_o value was verified by calculating the in-depth stress component (σ_{33}) which should vanish if the plane stress condition is satisfied. The stress-strain analysis was done using the classic Hauk's algorithm (Hauk et al., 1982). The stress conversion was carried out using an elastic modulus of E=210 GPa and Poisson's ratio,ν=0.3. The estimated standard deviation of RS and strains was calculated following the procedure described in (Rudnik and Cohen, 1986). The RS were not corrected for the material removal. The possible effect of sample geometry (curvature of the cylinder) on the peak position, and thus RS, was tested by taking measurements on a stress-free sample with an identical geometry. The stress-free standard was prepared by painting a 100 μm thick layer of iron powder (particle size =10μm) on a 9.53 mm (3/8") diameter Teflon rod. The stresses measured on this standard were practically 0 (within the error bars).

3. RESULTS

Figure 1 shows the residual stress distribution as a function of radia-

---

Nomenclature:

A1 = SAE 52100 carbonitreded, high austenite
AC2 = SAE 52100 carbonitreded, high aust. + carbides
AD = artificial defects
DER = dark etching regions
E = elastic module
L_{10}, L_{50} = lives @10 and 50 % failure probability respect.
N = number of contact or stress cycles
RA = retained austenite
RAT = retained austenite transformed
RB = rough balls
RCF = rolling contact fatigue
RD = rolling direction
RS = residual stresses
RIII = SAE 52100 sample, tempered@240°C
WEB = white etching bands
a = semiminor axis of the contact ellipse
b = semimajor axis of the contact ellipse
d_o = unstressed lattice spacing
p_o = peak contact pressure
r^2 = correlation degree
Δσ = residual stress increase
β = Weibull slope
γ → α' = austenite into martensite transformation
θ = Bragg angle
σ^r = residual stresses
σ^r_c = circumferential residual stresses
σ_{11} ; σ_{22} ; σ_{33} = circumf., axial and normal stresses
τ = penetration depth
ν = Poisson's ratio
ψ = tilts for RS measurements

depth for specimens type RIII, A1 and AC2 in the unworn state, σ_{11} corresponds to the axial stresses (along the axis of the specimen) and σ_{22} corresponds to the circumferential stresses. These RS are due to the heat treatment and grinding operations. The maximum surface RS are equal to: a) σ_{11} = - 570 MPa and σ_{22} = - 368 MPa for specimen RIII, b) σ_{11} = - 474 MPa and σ_{22} = - 361 MPa for specimen A1, and c) σ_{11} = - 528 MPa and σ_{22} = - 398 MPa for specimen AC2. Also shown in Fig.1 are the initial RS for samples RI and RII with σ_{11} = -548 MPa, σ_{22} = -262 MPa and σ_{11} = -479 MPa, σ_{22} = -277 MPa, respectively. The magnitude of axial residual stresses was higher than the circumferential stresses at the surface for all samples and at 35 μm for RIII and 40 μm for A1 and AC2. The amount of RA at the surface was ~3.6, ~38 and ~20% for specimens RIII, A1 and AC2, respectively. At a depth of 75 μm the axial and the circumferential stresses have turned tensile for all the materials. The tensile stresses seem to extend deeper into the specimen type RIII, and return to compressive at 150 μm for A1 and AC2. Error bars for RS measurements have an average value lower than 80 MPa for both σ_{11} and σ_{22}, and for most of the tests this value was much lower (approximately 45 MPa).

Figures 2-4 show the variation of the RS components σ_{11} and σ_{22} in specimens RIII, A1 and AC2. This is showed as a function of life expressed by N, the number of contacts or loading cycles and for different depths, i.e. d = 0, 35, 80, 140 and 200 μm. The present work has concentrated on the phenomena taking place near surface regions. One can observe the build up of the surface compressive RS with the number of cycles. For specimens type A1 and AC2 there is an increase in the RS up to N ~ 10^7. At this point a change towards less compressive surface RS is observed. This behavior is experienced by both the higher axial residual stress, σ_{11}, and the circumferential stress, σ_{22}. The specimens type RIII show a continuous increase of the axial compressive stresses at the surface, and the circumferential stresses show a decrease starting at N ~ 10^5. The RS at depths higher than ~ 140 μm (refer to the keys in Figures 2-4) are considerably lower in magnitude and tensile, i.e. $\sigma_{11}, \sigma_{22} \leq 200$ MPa.

Figure 5 shows the volumetric fraction of RA present at the surface in unworn specimens type RI, RII, RIII, A1 and AC2. For the carbonitrided specimens, i.e. A1 and AC2, the amount of RA is also shown at 40 and 100 μm. The RA content at the surface for the tempered sapecimens RI, RII and RIII was uniformly low and approximately equal to 8, 16, and 4%, respectively. Figures 6 and 7 show the amount of retained austenite transformed (RAT) as a function of life for specimens type A1 and AC2, and at different depths under the wear tracks. The RA decays very rapidly at the surface and then, becomes approximately constant, at around N = 10^6 cycles in specimen type A1, and N = 10^7 in specimen type AC2. The transformation rate at 100 μm is higher than at 40 μm for A1 and AC2, but in both cases are far from completion, reaching a maximum for these tests of near 50% at N = 10^6 contacts.

Figures 8 shows the results of Weibull analyses, i.e. failure probability versus life of the RCF experiments, of specimens type RI, RII and RIII. Figure 9 presents similar analysis for specimens type A1 and AC2. These results are summarized in Table III which shows the L_{10} and L_{50} lives, β - the Weibull slope, and r^2 - the degree of correlation. In all cases the Weibull slopes were lower than 3.3, which is similar to the results obtained with smooth, unindented specimens (Glover, 1982).

4. DISCUSSION

The large compressive RS observed at the surface of unworn martensitic bearing steels, see Fig. 1, result from manufacturing operations. The residual stress vs. depth profiles due to heat treatment and grinding indicate that the hoop stresses (σ_{22}) are shifted by approximately 100 MPa towards less compressive values. This difference diminishes with depth and disappears at around 80 μm. It has been shown that this effect is reduced by shot peening which has no directional effect (Castanhola Batista et al., 1993).

The subsequent evolution of these stresses has long been ascribed to the volumetric change associated with the stress-assisted/strain-induced γ-α' transformation (5,22). This transformation has been indicated to be accompanied by a 3 - 4% (5,23) volume expansion, and it has been estimated (Hahn et al., 1987) that a complete transformation in a steel with a 12.5% retained austenite content may result in an increase in the compressive residual stress level of up to σ' = -400 MPa. Our observations indicate that in the specimens type A1, the transformation at the surface appears to have saturated at a level of 75%; this could be due to high RA stability, and also RS which increase the energy necessary to drive the transformation. The surface RS for this material increase ($\Delta\sigma$ = - 500 MPa) up to N ~ 10^7 cycles, declining thereafter. Specimens type AC2, which show an increase in the RA content with depth, i.e. ~20% at the surface versus ~39% at 100 μm for the unworn condition, show a smaller increase in the RS at the surface ($\Delta\sigma$ = - 300 MPa) up to N ~ 10^7 cycles declining after this value. This lower increase in RS may be due to a lower RA content at the surface in the unworn condition. The percent of RAT as a function of the number of cycles follows the pattern observed for A1 specimens, but in this case reaches 85% of transformed RA at the surface. Similarly, specimens of type RIII with the lowest percent of RA at the surface, i.e. ~4%, show an increase ($\Delta\sigma$ = - 250 MPa) in the surface RS up to N ~ 10^5 contacts; at around N ~ 5x10 contacts, 50% of the RA is transformed.

The volumetric change produced during the decomposition of the RA contributes to the generation of compressive residual stresses. The contribution of this phase transformation to the RS build-up is not linearly related to the RA content, and may be of similar magnitude to the RS generated by inhomogeneous kinematic-plastic deformation. Specimens with a large difference in their retained austenite content, such as RIII (~4%) and A1 (~38%), are subjected to similar changes in the surface hoop RS, $\Delta\sigma$ = - 250 MPa for RIII versus $\Delta\sigma$ = - 380 MPa for A1. The decrease in magnitude of RS observed at higher numbers of stress cycles, i.e. N > 10^7, may be the result of softening due to a decay of the martensite, which produces a net reduction in the volume (tensile stresses).

The carbonitrided steels, A1 and AC2, show higher RA concentrations at the surface, i.e. ~38 and ~20% respectively. Their L_{50} lives are higher than those measured in the tempered specimens. Among these, the specimens type RII which have the largest L_{50} life, i.e. L_{50} = 29.17x10^6, are also the ones with the highest content of RA at the surface, i.e. ~ 16%. The present work agrees with early observations (Maeda and Tsushima, 1994, Glover, 1982) in that there would be a direct correlation between the percent retained austenite and the RCF.

Even though RA transformation and RS development are apparently not directly coupled, both contribute to RCF life enhancement. It has been shown (Broszeit, 1984; Harris, 1992) that compressive RS are beneficial, whatever their nature may be. On the other hand RA, when not transformed is present as a fine mixture with martensite enhancing the material toughness. This may be the most important benefit of RA since RCF life was roughly doubled when comparing A1 or AC2 against RIII lives, while the increase in RS are of the similar magnitude.

5. CONCLUSIONS

The heat treating processes applied to SAE 52100 steel rods (Table II) resulted in different distributions of RS and RA in the sub-surface regions

(up to 200 μm) The RCF induced the microstructural changes (austenite to martensite transformation) and the RS redistribution at all tested depths under the surface

The residual stress vs. depth profiles due to thermomechanical treatment for carbonitrided samples A1 and AC2 were almost identical. The hoop and axial stresses showed the same distribution, with the hoop stresses shifted by approximately 100 MPa towards the less compressive values. The tempered samples (e.g., RIII) showed different stress profiles but had the same magnitude of compressive stresses at the surface as the carbonitrided samples in the range -400 to -600 MPa.

The rolling contact deformation induced the transformation of RA and resulted in the redistribution of stresses in the sub-surface regions. Rolling contact cycling up to $N \approx 10^7$ cycles increased the magnitude of compressive stresses at the surface; further cycling resulted in lowering the compressive residual stresses. The rates of increase and the subsequent decrease of stresses were higher for the carbonitrided samples as compared with the tempered ones. The stresses at higher depths (above 80 μm for the tempered RIII and above 40 μm for the carbonitreded A1 and AC2 samples) do not change significantly with the number of cycles and oscillate in the range of -200 to 200 MPa.

Carbonitriding resulted in higher volumetric fractions of RA than the tempering process. Samples of type AC2 showed a lower RA content than A1 at the surface but at higher depths (approx. 100 μm) both types of samples had the same RA content (35-40%). The austenite at the surface of A1 and AC2 transformed at high rates and reached a stable level after 10^6-10^7 cycles when 80% of the RA was transformed. The transformation kinetics were different for different depths; the transformation rate was higher at 100 μm below the surface than at 40 μm. This is in agreement with the location of the most unfavorable shear stresses assisting the transformation around $a/2 \approx 90$ μm.

The carbonitrided samples A1 and AC2 showed the highest fatigue resistance. They had the same distribution and magnitude of compressive residual stresses in the surface regions. A1 showed a superior fatigue resistance which was attributed to the highest volumetric fraction of RA at the surface.

The carbonitriding process for manufacturing of the A1 sample proved to be superior in that it provided for the highest resistance to RCF failure.

6. ACKNOWLEDGMENTS

The authors would like to thank Dr. John Beswick and Aidan Kerrigan from SKF for providing the specimens used in the present research effort. Thanks are due to Mrs. Mary-Joe Liston from NTN-Bower Corp. for suggesting the use of the 5-ball-rod technique. Mr. Ricardo C. Dommarco would like to acknowledge the support provided by Dr. F. Lantos and Mr. O. Quiroga from the Centro Argentino de Tribologia. Partial funding for this project was provided by the National Science Foundation. This project was partially sponsored by the Assistant Secretary for Energy Efficiency and Renewable Energy, Office of Transportation Technologies, as part of the High Temperature Materials Laboratory User Program, Oak Ridge National Laboratory, managed by Lockheed Martin Energy Research Corporation for the U.S. Department of Energy under contract number DE-AC05-96OR22464.

7. REFERENCES

Barski, T., 1994, "The formation of residual stresses in grinding," *Proceed. 4th. Internat. Conf. on Residual Stresses*, pp. 913-915, June 8-14, Baltimore, USA. Published by the Society for Experimental Mechanics (SEM).

Bastias, P. C., Gupta, V., Hahn, G. T., Rubin, C. A., and Leng, X., 1994, "Analysis of Rolling Contact Spall Life in 440C Bearing Steels", *Wear*, 171, pp. 169-178.

Batista, A. C., Dias, A. M., Le Flour, J. C., and Lebrun, J. L., 1994 June 8-14, "Residual stresses and damage evolution during pitting tests of automotive gears," *Proceed. 4th. Internat. Conf. on Residual Stresses*, pp. 1062-1070, Baltimore, USA. Published by the Society for Experimental Mechanics (SEM).

Broszat, E., Adelmann, J., Zwirlein, O, 1984, "Influence of internal stresses on the stressing of material in components subjected to rolling-contact loads," *ASME Journal of Tribology*, Vol.106, pp. 499-504.

Castanhola Batista, A., Morão Dias, J. C. Le Flour, and J. L. Lebrun, 1993, "Residual Stresses Evolution During Pitting Tests of Automotive Gears," *Residual Stresses - European Conference on Residual Stresses*, (ed. Hauk, V., Hougardy, H. P., Macherauch, E. and Tietz, H. D.), Nov. 1992, Frankfurt a. M., Germany, DGM Informationsgesellschaft Verlag, pp. 425-432.

Cullity, B. D., 1978, "Elements of x-ray diffraction," 2nd edition, Addison-Wesley, Reading, MA.

Dölle, H. and Hauk, V., 1977, "System of possible lattice strain distributions on mechanically loaded metallic materials, " (in German) *Zeitschrift fuer Metallkunde*, Vol. 68, pp. 725-728.

Glover, D., 1982, "A ball-rod rolling contact fatigue tester," *Rolling Contact Fatigue Testing of Bearing Steels, ASTM STP-771* (ed. J. J. C Hoo), pp.107-124, ASTM, Philadelphia.

Hahn, G. T., Bhargava, V., Rubin, C. A., Chen, Q., and Kim, K., 1987, "Analysis of rolling contact residual stresses and cyclic plastic deformation of SAE 52100 steel ball bearings," *ASME Journal of Tribology*, Vol. 109, pp. 618-626.

Harris, T.A., Ragen, M.A., Spitzer, R.F., 1992, "The effect of hoop and material residual stresses on the fatigue life of high speed, rolling bearings," *STLE Tribology Transactions*, Vol.35, 1, pp. 194-198.

Hauk, V. M., Oudelhover, R. W. M., and Vaessen, G. H. J., 1982, "The state of residual stress in the near surface region of homogeneous and heterogeneous materials after grinding," *Metall. Trans. A.*, Vol. 13A, pp 1239-44.

Johnson, K. L., and Jeffries, J., 1963, "Plastic flow and residual stresses in rolling and sliding contact," *Proc. Int. Mech. Eng.*, Symposium on Rolling Contact Fatigue, V. 177, pp. 50-.

Liston, M.-J., 1995, Personal Communication, NTN-Bower, Troy, MI.

Maeda, K., Tsushima, N., 1994, "Influence of preexisting residual stress on rolling bearing fatigue life," *Proceed. 4th. Internat. Conf. on Residual Stresses*, pp. 899-906, June 8-14, Baltimore, USA. Published by the Society for Experimental Mechanics (SEM).

Noyan, I. C., and Cohen, J. B., 1987, "Residual stress, measurement by diffraction and interpretation," Springer-Verlag, New York.

Österlund, R., and Vingsbo, O., 1980, " Phase changes in fatigued ball bearings," *Metall. Trans. A*, Vol. 11A, pp. 701-707.

Porter, D. A., and Easterling, K. E., 1981, "Phase Transformations in Metals and Alloys," Chapman & Hall, New York, p. 389.

Rudnik, P. and Cohen, J. B., 1986, "Errors due to counting statistics in the triaxial strain (stress) tensor determined by diffraction," *Adv. X-ray Anal.*, Plenum Press, New York, Vol. 29, pp. 79-88.

Schlicht, H., Schreiber, E., and Zwirlein, O., 1988, "Effects of material properties on bearing steel fatigue strength," *Effects of Steel Manufacturing Process on the Quality of Bearing Steel, ASTM STP 987* (ed. J. J. C. Hoo), pp. 81-101, ASTMP, Philadelphia.

Swahn, H., Becker, P. C., and Vingsbo, O., 1976, "Martensite decay during rolling contact fatigue in ball bearings," *Metall. Trans. A*, Vol. 7A,

pp. 1099-1110.

Tricot, R. Monnot, J. and Lluansi, M., 1972, "How microstructural alterations affect fatigue properties of 52100 steel," *Metals Engineering Quarterly*, Vol. 12, pp. 39-47.

Voskamp, A. P., 1994, "Rolling contact fatigue and the significance of residual stresses," *Proceed. 4th. Internat. Conf. on Residual Stresses*, pp. 913-915, June 8-14, Baltimore, USA. Published by the Society for Experimental Mechanics (SEM).

Voskamp, A. P., Österlund, R., Becker, P. C., and Vingsbo, O., 1980, "Gradual changes in residual stress and microstructure during contact fatigue in ball bearings," *Metals Technology*, Vol. 7, pp. 14-21.

Voskamp, A. P., 1985, "Material response to rolling contact loading," *ASME Journal of Tribology*, Vol. 107, pp. 359-366.

Yajima, E., Miyazaki, T., Sugiyama, T., and Terajima, H., 1974, "Effects of retained austenite on the rolling fatigue life of bearings steels," *Trans. JIM*, Vol. 15, pp. 173-179.

Zwirlein, O., and Schlicht, H., 1982, "Rolling contact fatigue mechanisms - accelerated testing versus field performance," *Rolling Contact Fatigue Testing of Bearings - ASTM STP 771* (ed. Hamrock, B. J. and Dowson, D. J.), pp. 358-379, ASTM, Philadelphia.

Table I. Chemical composition of AISI 52100 specimens (wgt.%).

C	Si	P	Mo	Mn	Cr	Fe
0.75 - 1.10	1.0 max.	≤ 0.015	0.5 max.	1.2 max.	0.5 - 2.0	bal.

Table II. Heat treatments.

Specimen ID	Heat Treatment	Surface Hardness HRC (Knoop 500)
RI	Martensitic hardened - tempered @ 160 °C/1.5 hrs.	62.5
RII	Martensitic hardened - tempered @ 200 °C/1.5 hrs.	60.5
RIII	Martensitic hardened - tempered @ 240 °C/1.5 hrs.	58.5
A1	Martensitic hardened and tempered @ 200 °C/1.5 hrs. Carbonitrided @ 780-900 °C/1-10 hrs in an atmosphere with a C activity between 0.9 and 1.1 and a N potential between 0.1 and 0.6% N	65/(850)
AC2	Same as A1 on a bar with different thickness.	66/(880)

Table III. Summary of the RCF tests on SAE 52100.

Sample Type	Life x (10^6 cycles)		Weibull Slope β	Correlation Factor r^2
	L_{10}	L_{50}		
RI	14.98	26.90	3.2719	0.9194
RII	14.10	29.17	2.5526	0.8617
RIII	10.93	20.00	3.2211	0.9635
A1	18.79	46.90	2.0293	0.7914
AC2	15.43	35.59	2.2548	0.9594

DISCLAIMER

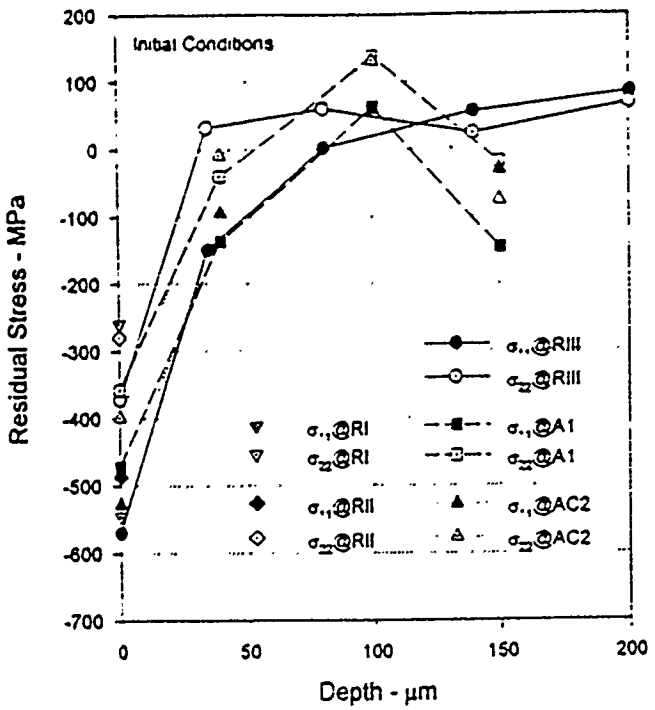

Figure 1. Initial RS (unworn) as a function of depth for the three materials studied by x-ray diffraction: RIII, A1 and AC2. Also RS at surface for samples RI and RII. Refer to Table II for heat treatments.

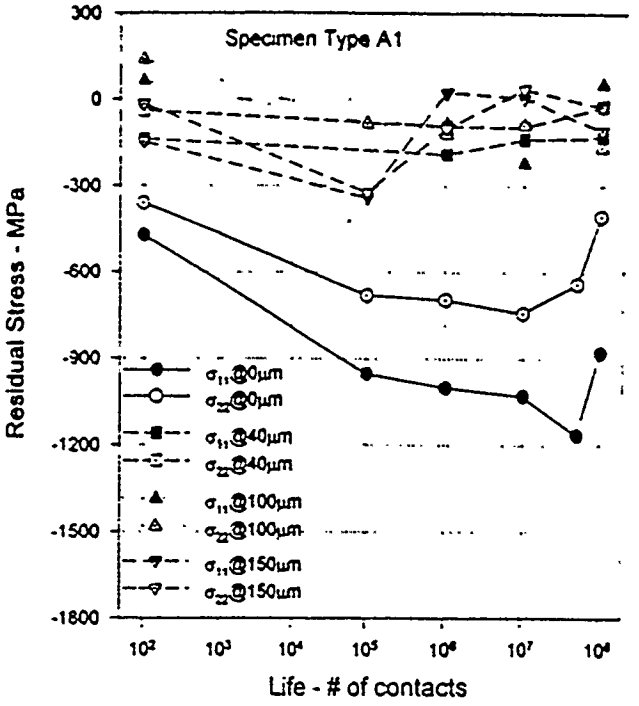

Figure 3. Residual stresses as a function of life for the A1 specimens. RS σ_{11} (axial) and σ_{22} (long.) are shown for different depths: 0 μm (surface), 40 μm, 100 μm and 150 μm.

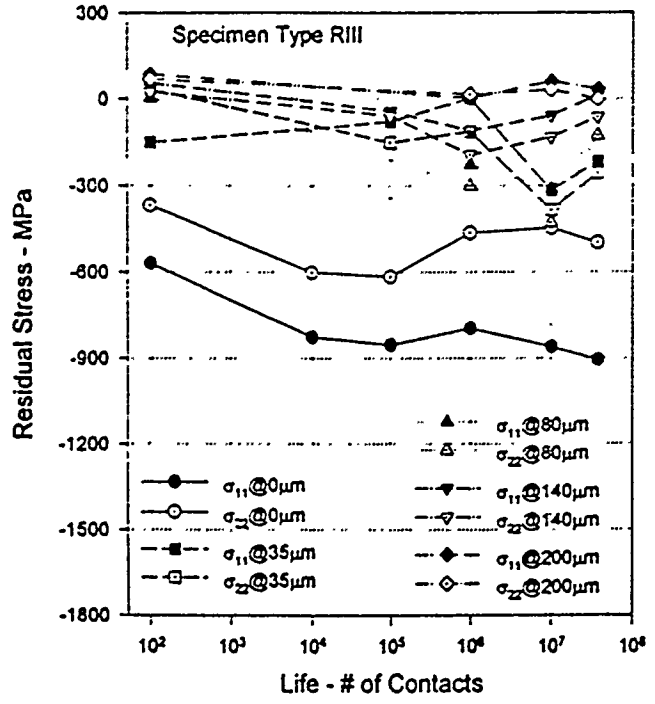

Figure 2. Residual stresses as a function of life for the RIII specimens. RS σ_{11} (axial) and σ_{22} (long.) are shown for different depths: 0 μm (surface), 35 μm, 80 μm, 140 μm and 200 μm.

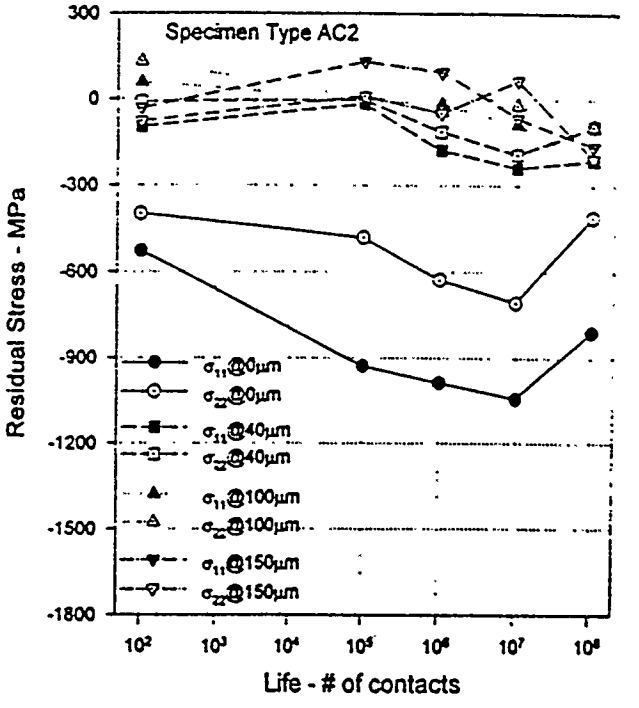

Figure 4. Residual stresses as a function of life for the AC2 specimens. RS σ_{11} (axial) and σ_{22} (long.) are shown for different depths: 0 μm (surface), 40 μm, 100 μm and 150 μm.

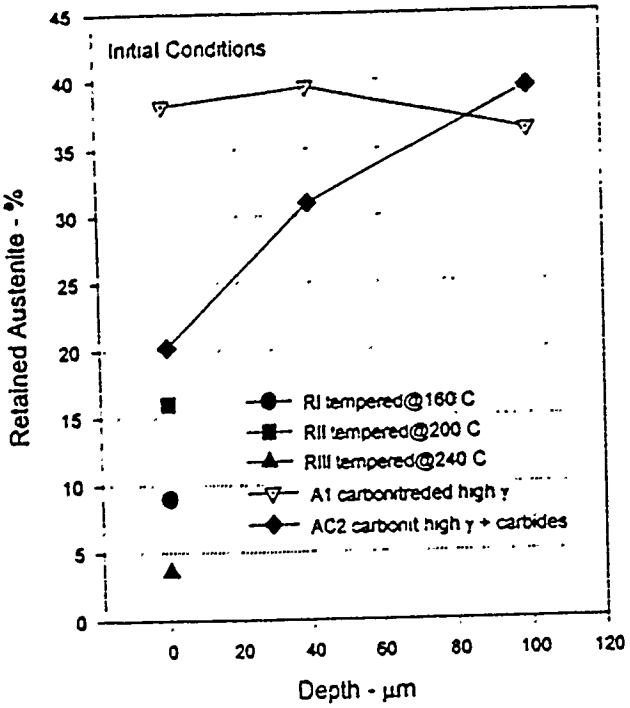

Figure 5. Initial RA (unworn) as a function of depth for materials RIII, A1 and AC2. Also RA at the surface for samples RI and RII. Refer to Table II for heat treatments.

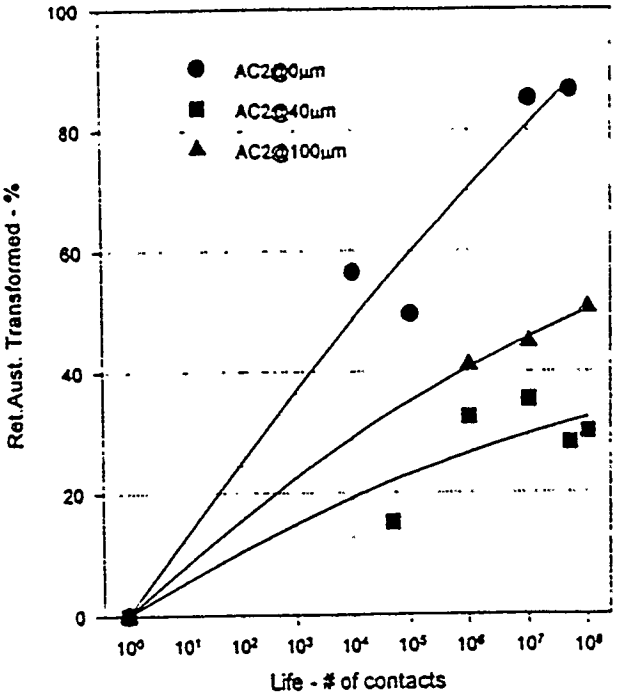

Figure 7. Ret. austenite transformed as a function of life for the AC2 sample at different depths: 0 µm, 40 µm, 100 µm. The maximum RA content at each depth, see Fig. 5, is used as a reference.

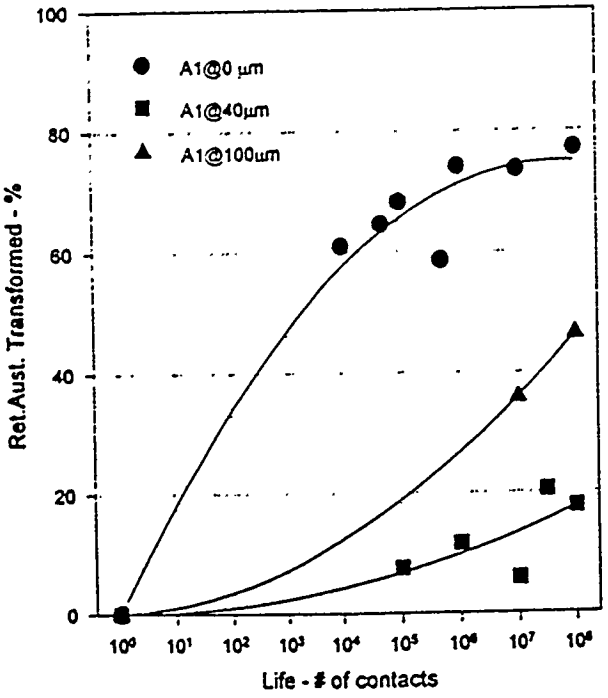

Figure 6. Retained austenite transformed as a function of life for the A1 sample at different depths: 0 µm, 40 µm, 100 µm. The maximum content at each depth, see Fig. 5, is used as a reference.

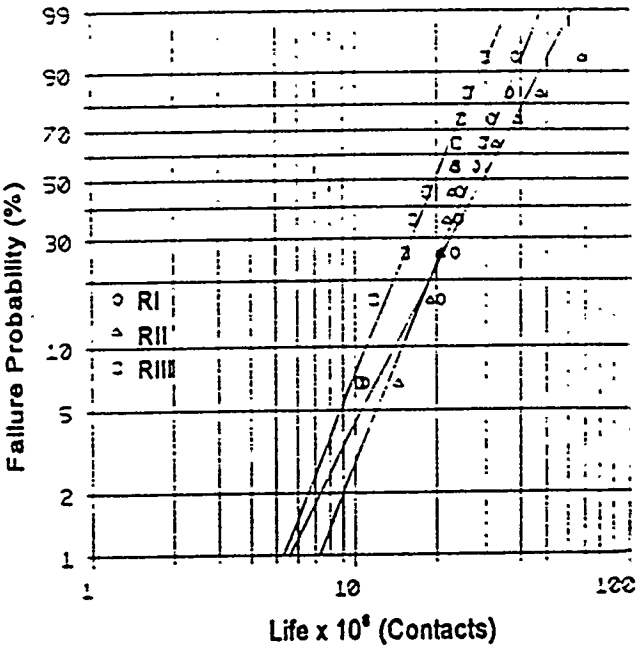

Figure 8. RCF failure probability as a function of life for the conventionally heat treated samples: O RI, tempered at T = 160°C; Δ RII, tempered at T = 200°C; □ RIII, tempered at T = 240°C.

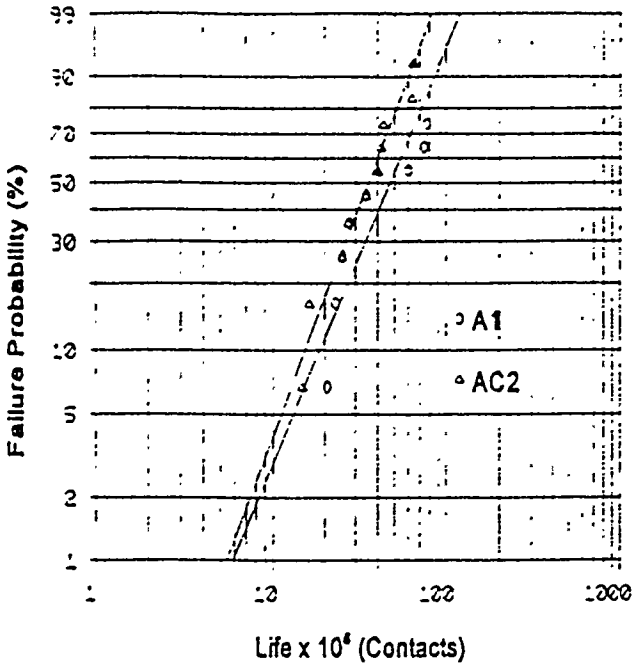

Figure 9. RCF failure probability as a function of life for the carbonitrided samples: O A1, carbonitreded (high austenite) and ▵ AC2, carbonitreded (high austenite + carbides).